PHYSICAL REVIEW A VOLUME 17, NUMBER 4 APRIL 1978

Optical coherent transients by laser frequency switching

Azriel Z. Genack and Richard G. Brewer
IBM Research Laboratory, San Jose, California 95193
(Received 20 December 1977)

A simple method for observing coherent optical-transient phenomena is described. Effects such as photon echoes and free induction decay (FID) should allow studies of the dynamic properties of atoms, molecules, and solids on a time scale ranging from milliseconds to ~50 ps. The frequency of a cw dye laser is switched with an intracavity electro-optic modulator, producing in an external sample coherent transients which are detected in the forward beam. Measurements of long dephasing times are possible, as in FID, because the laser can oscillate indefinitely at the new frequency following a step-function switching pulse. Measurements of short decay times are also practical because the switching time is not restricted by the laser gain or cavity ringing time. In addition, the dye's dephasing time of a few picoseconds or less is too rapid to interfere with these observations. Since the pulse sequence can be preselected, the entire class of coherent optical transients is accessible. The method thus incorporates all of the advantages inherent in Stark switching, including heterodyne detection and high sensitivity, without being restricted to Stark-tunable sytems. Laser frequency switching is discussed also in terms of a theoretical model which exposes the time-dependent properties of a phase-modulated cavity mode. Dephasing studies have been carried out thus far in atomic and molecular gases and low-temperature solids containing inorganic impurity ions or large organic molecules. The utility of the FID effect is emphasized where precise dephasing times are obtained from time-frequency Fourier transformation of FID signals using a digital computer. The first quantitative and detailed test of FID theory is provided by these experimental techniques.

I. INTRODUCTION

Optical coherence phenomena such as photon echoes[1] and free induction decay[2] (FID) have been detected recently using a *frequency-switched* cw laser.[3] The advantages of this new technique, which have been described briefly in a recent Letter,[3] include simplicity and versatility. As a result, the general class of coherent optical transients[4] may now be observed in atoms, molecules, and solids, and in a way which closely resembles the spin transients of pulsed nuclear magnetic resonance.[5] Since specific dephasing and dissipative processes of coherently prepared systems can be examined selectively, these dynamic studies offer a new and attractive alternative to the traditional line-broadening technique used so extensively in the pre-laser era.

In this paper, various aspects of laser frequency switching are treated. First, the characteristic behavior of a cw laser subject to arbitrary frequency or phase modulation is examined. Even though a large literature[6] exists on amplitude and frequency modulation of lasers, many of the properties uncovered here are not appreciated generally. Therefore, an appropriate theoretical model of a frequency-switched laser is developed.

The experimental details of laser frequency switching are presented also, and limits are predicted for decay-time measurements in the very fast or very slow time regions. Last, some applications of laser frequency switching are considered. The utility of the FID effect is emphasized where precise dephasing times are obtained from time-frequency Fourier transformation of FID signals using a digital computer.

II. BASIC CONCEPT

Consider a single-mode cw laser beam of frequency Ω which initially excites an atomic-gas sample under steady-state conditions. For a Doppler-broadened atomic line shape, as in Fig. 1, the atomic group having longitudinal velocity v_z will be excited resonantly. These atoms are coherently prepared since each excited two-level quantum system is in coherent superposition. The entire collection of excited atoms constitutes a phased array of dipoles which can emit or absorb coherent light. The well known atom-field interaction is described by the Maxwell and Schrödinger wave equations, and the relevant theory can be found elsewhere.[7,8]

Now imagine that the laser frequency is abruptly switched to a new value Ω'. The initial velocity group v_z, which is no longer resonant with the applied field, radiates a coherent beam of light in the forward direction—the FID effect. Simultaneously, a second velocity group v_z' is excited coherently; this group exhibits the nutation effect. If the laser is frequency-switched twice in succession in two brief pulses, the velocity group v_z' emits a photon echo in the forward direction. Evidently, by varying the pulse sequence the en-

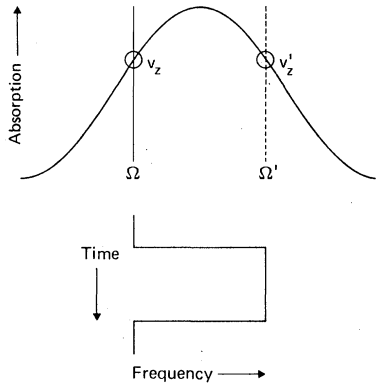

FIG. 1. Observation of coherent optical transients by laser frequency switching is illustrated for the case of a Doppler-broadened line. When the laser frequency is suddenly switched from Ω to Ω′, the initially prepared velocity group v_z is no longer in resonance and radiates the FID signal. Simultaneously, the group v_z' comes into resonance with the new laser frequency Ω′ and exhibits the nutation effect. When the laser frequency is switched twice by two successive pulses, the group v_z' emits the photon echo.

tire class of coherent optical transients can be observed in this manner.

Note that heterodyne detection occurs automatically because the coherent light radiated by the sample overlaps the laser beam in space and time and the two are displaced in frequency due to the laser frequency shift. Thus, the sample retains memory of the initial laser frequency in the preparative stage whereas the laser at its new frequency acts as a local oscillator.

Laser frequency switching obviously resembles Stark switching.[9] In the latter, the molecule's transition frequency is switched by a dc electric field pulse while the laser frequency remains fixed. From the standpoint of the atom, the time-dependent interaction is the same in the two cases, and the two techniques are equivalent. However, laser frequency switching is not restricted to Stark tunable systems, and with a cw dye laser,[10] the broad tuning range permits quite general studies in atoms, molecules and solids.

We note that a variant of the above ideas has been reported by Hall[11] who observed optical transients from a methane sample located inside the cavity of a frequency-shifted 3.39-μm He-Ne laser.

III. SWITCHING THEORY

The possibility of frequency shifting a laser by means of an intracavity electro-optic element was mentioned previously by Yariv.[12] Using a steady-state argument, he calculated the laser frequency shift which accompanies a change in the refractive index of the electro-optic crystal and corresponds to a new optical length of the laser cavity. We prefer to examine the time-dependent behavior of laser frequency switching in order to clarify the dynamic aspects of the problem, particularly as they affect the observation of coherent-optical-transient phenomena. The unique role which dye lasers play in this regard will be discussed in Sec. IV C.

We consider in Fig. 2 a cavity of optical length L which initially contains a standing-wave optical field:

$$E(z,t)=E_0(e^{i(\omega t-kz)}+e^{i(\omega t+kz)})+\text{c.c.} \tag{1}$$

of angular frequency

$$\omega=\nu 2\pi/T\ , \tag{2}$$

ν being a large integer. The light wave therefore circulates through the cavity in the round-trip time

$$T=2L/c\ .$$

Assume that the cavity introduces no loss and that an electro-optic phase modulator situated next to one end mirror imposes a time-dependent phase variation $\phi(t)$ on the light wave.

The nature of the problem can be illustrated by considering only one running wave

$$E(z,t)=E_0e^{i(\omega t-kz)}\ , \tag{3}$$

of Eq. (1), as it propagates through a modulator located between $z=0$ and $z=z_x$ where its thickness $z_x \ll L$. We assume for the moment that the phase of this light wave

$$\phi=kz_x \tag{4}$$

at the position $z=z_x$ is modulated by a ramp function

$$\begin{aligned}\phi(t)&=\dot{\phi}t, \quad 0<t<t_1\\ \phi(t)&=\dot{\phi}t_1, \quad t_1<t\end{aligned} \tag{5}$$

as indicated in Fig. 3 where the phase time derivative $\dot{\phi}$ is a constant. The ramp begins at $t=0$ and reaches its final value at $t=t_1$. Also note that

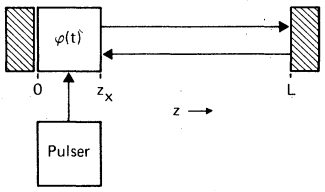

FIG. 2. Schematic of an optical cavity of length L containing a phase modulator $\phi(t)$ of thickness z_x adjacent to one end mirror.

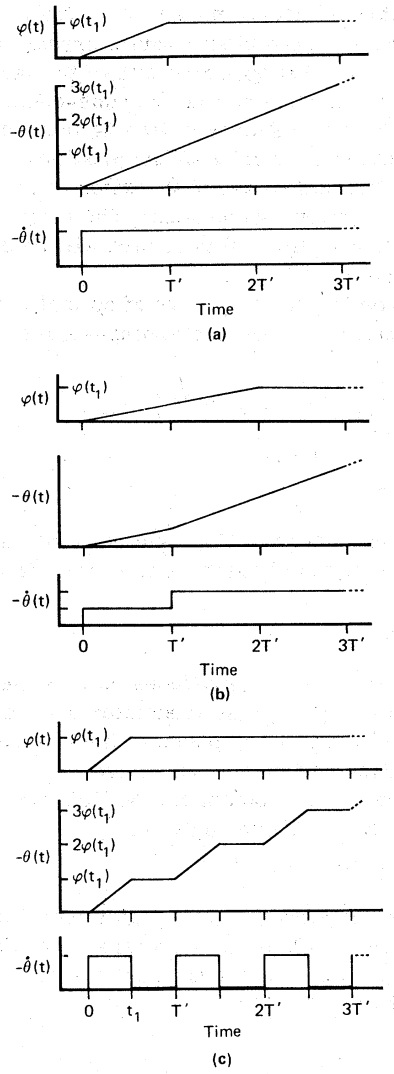

FIG. 3. Graphical representation of the periodic behavior of an electro-optically phase modulated cavity mode for three different ramp times t_1. The top curve $\phi(t)$ shows the phase modulation as a function of time; the second curve $\theta(t)$ is the resulting phase of the light wave; and the third curve $\dot{\theta}$ is its time derivative which illustrates the instantaneous frequency shift. Time is measured in units of the new cavity round-trip time T'. In (a), $t_1 = T'$ and the mode is shifted in frequency by $-\dot{\phi}$. In (b), $t_1 = qT'$, where the integer $q = 2$, and the frequency is shifted twice. In (c), $t_1 < T'$ and more than one mode is produced as explained in the text.

the phase excursion (5) involves a double pass through the modulator since it is adjacent to one end mirror as in Fig. 2.

Taking the time derivative of (4), we can write the phase variation (5)

$$\phi(t) = \dot{\phi}t = 2(\omega/c)z_x\dot{n}t \tag{6}$$

in terms of the modulator's refractive index n where the factor of 2 accounts for the double passage mentioned above. The field at $z = z_x$ then becomes

$$E(z_x,t) = E_0 e^{i(\omega-\dot{\phi})t - ikz_x}, \quad 0 < t < t_1 \tag{7a}$$

$$E(z_x,t) = E_0 e^{i[\omega t - \phi(t_1)] - ikz_x}, \quad t_1 < t < T' \tag{7b}$$

where the new cavity round-trip time is T'. Equation (7a) indicates that the initial frequency ω is shifted to the new value $\omega - \dot{\phi}$ in the interval $0 < t < t_1$. From (6), we see that the frequency shift

$$\dot{\phi} = 2(\omega/c)z_x\dot{n}$$

takes the form of a Doppler shift if we associate $z_x\dot{n}$ with the effective translation velocity of the modulator. In the Appendix, frequency shifting is treated for the analogous case where the end mirror of the cavity introduces a Doppler shift due to its motion. It is also evident from (6) that for times $t > t_1$, the phase change $\phi(t_1)$ implies the additional retardation

$$\Delta T = \phi(t_1)/\omega = 2(z_x/c)\dot{n}t_1 \tag{8}$$

each time the wave train passes through the modulator twice. Thus, the light wave circulates indefinitely at the new round-trip time

$$T' = T + \Delta T. \tag{9}$$

We see from this argument that the initial periodic behavior is not affected by the above phase disturbance. Only the period is changed from $T \to T'$, and this change depends on the final value $\phi(t_1)$, not on the phase-time path. Furthermore, this consideration is not restricted to a ramp function, but would apply in general for $\phi(t)$ of arbitrary form.

Since the phase-modulated field is periodic in the interval T', it can be expressed as a Fourier series

$$E(x) = \sum_{\nu=-\infty}^{\infty} a_\nu e^{i\nu x}, \quad x = 2\pi t/T' \tag{10a}$$

where the amplitude of the νth mode is given by

$$a_\nu = \frac{1}{2\pi}\int_{-\pi}^{\pi} E(x)e^{-i\nu x}\,dx = a_{-\nu}^*, \quad \nu = 0, \pm 1, \pm 2, \ldots, \tag{10b}$$

its frequency is

$$\Omega = \nu 2\pi/T', \tag{10c}$$

and the new round-trip time from (8) and (9) is

$$T' = T + \phi(t_1)/\omega. \tag{10d}$$

Whereas the mode frequency depends on $\phi(t_1)$, the mode amplitude depends on the specific form of $\phi(t)$. In general, several modes might be genera-

ted by phase switching. Some important cases where one mode persists are treated below.

To proceed further, specific forms of $\phi(t)$ must be assumed and reveal still other features of frequency switching. We continue to focus attention on one running wave, Eq. (3), at the position $z = z_x$ and again assume that it is phase modulated by the ramp function Eq. (5). It will be convenient to express the periodic behavior of the running wave prior to phase switching by

$$E(t) = E(t - T), \quad t < 0$$

and after phase switching by

$$E(t) = E(t - T)e^{-i\phi(t)}, \quad t > 0 \tag{11}$$

where the round-trip time changes from $T \to T'$ due to the phase factor $e^{-i\phi(t)}$, consistent with (7).

We may also express the phase-modulated field in the form

$$E(t) = E_0 e^{i[\omega t + \theta(t)]}$$

where $\theta(t)$ is the resulting phase. Inserting the above expression into (11) yields the phase relation

$$\theta(t) = \theta(t - T) - \phi(t). \tag{11a}$$

Equation (11a) states that the phase $\theta(t)$ at time t is given by the phase at the earlier time $t - T$ plus any additional phase modulation. It is apparent that the phase advances each round trip according to (11a). These ideas are illustrated in Fig. 3 where $\theta(t)$ and its time derivative $\dot{\theta}(t)$ are shown for three different cases.

We now discuss three cases which differ only in the time t_1 needed for the phase ramp to reach its final value $\phi(t_1)$.

A. Case 1: phase ramp, $t_1 = T'$

Assume that the initial field at position $z = z_x$ is

$$E(t) = E_0 e^{i\omega t}, \quad t < 0 \tag{12}$$

before phase switching and that the ramp phase function

$$\begin{aligned} &\phi(t) = \dot{\phi}t, \quad 0 < t < T' \\ &\phi(t) = \phi(t_1) = \dot{\phi}T', \quad T' < t \end{aligned} \tag{13}$$

reaches its final value in one round trip at $t_1 = T'$. In Eq. (12) and hereafter we drop the constant phase factor e^{-ikz_x}. The simultaneous solution of (10c) and (10d) for $t_1 = T'$ yields

$$T' = \omega T/(\omega - \dot{\phi}), \tag{14}$$

so that the frequency of the initial mode $\nu = \omega T/2\pi$ is now

$$\Omega = \nu 2\pi/T' = \omega - \dot{\phi}. \tag{15}$$

The frequency is shifted downward by $\dot{\phi}$ due to the increase in the round-trip time, as expected.

The modulated field during the first round-trip interval becomes

$$E(t) = E_0 e^{i(\omega - \dot{\phi})t}, \quad 0 < t < T' \tag{16}$$

and from (11), in the second interval

$$E(t) = E(t - T)e^{-i\phi(T')}, \quad T' < t < 2T'. \tag{17}$$

Successive applications of (11) yield the behavior for all times as shown in the phase-time dependence of Fig. 3(a). However, since $E(t)$ is periodic in the interval T', knowledge of one period is sufficient.

Inserting (16) into (10b), we obtain the following Fourier amplitudes

$$\begin{aligned} &a_\nu = E_0, \quad \nu = (\omega - \dot{\phi})/(2\pi/T') \\ &a_\nu = 0, \quad \nu = (\omega - \dot{\phi})/(2\pi/T') \pm 1, \pm 2, \pm 3, \ldots . \end{aligned} \tag{18}$$

Hence, only one mode is produced. Since its frequency according to (15) is $\Omega = \omega - \dot{\phi}$, it is apparent that the frequency shift can be varied continuously by vaying $\dot{\phi}$.

From Eq. (16), we also see that the frequency shift occurs instantaneously at the onset of the ramp at $t = 0$ as indicated in the $\dot{\theta}$ curve of Fig. 3(a). Obviously, decreasing the cavity ringing time by relaxing the unit gain assumption will not affect this conclusion. However, the finite propagation time of light through the modulator ($z_x/c \sim 50$ psec) will introduce a distribution of phase shifts which will limit the switching time. A more detailed but more complicated boundary value solution of Maxwell's equations shows this behavior.[13]

This example also illustrates that once the initial mode is frequency switched, the new frequency persists as shown in the $\dot{\theta}$ curve of Fig. 3(a). This would not be the case if the modulator were external to the cavity as then the incident light would be frequency shifted only over the interval $0 < t < t_1$ when $\dot{\phi} \neq 0$. Thereafter, when $\dot{\phi} = 0$, the incident beam is not shifted. The numerous advantages of intracavity laser modulation, especially with dye lasers, will be taken up in Sec. IV.

B. Case 2: phase ramp, $t_1 = qT'$, $q = 1,2,3 \ldots$

Here, the modulation period extends over several round trips qT', where q is an integer. The initial condition (12) is assumed again, but now

$$\begin{aligned} &\phi(t) = \dot{\phi}t, \quad 0 < t < qT' \\ &\phi(t) = \phi(qT'), \quad qT' < t. \end{aligned} \tag{19}$$

Proceeding as in (14) and (15), the retardation introduced for q round trips leads to the final frequency

$$\Omega = \omega - q\dot{\phi} \tag{20}$$

for the initial mode $\nu = \omega T/2\pi$.

We have for the first round trip

$$E(t) = E_0 e^{i(\omega - \dot{\phi})t}, \quad 0 < t < T'$$

and by application of (11) for q round trips

$$E(t) = E_0 e^{i(\omega - q\dot{\phi})t}, \quad (q-1)T' < t < qT'. \tag{21}$$

Inserting (21) into (10b), the following Fourier amplitudes result:

$$\begin{aligned} &a_\nu = E_0, \quad \nu = (\omega - q\dot{\phi})/(2\pi/T') \\ &a_\nu = 0, \quad \nu = (\omega - q\dot{\phi})/(2\pi/T') \pm 1, \pm 2, \pm 3, \ldots . \end{aligned} \tag{22}$$

Here too, only one cavity mode appears where the frequency according to(20) is $\Omega = \omega - q\dot{\phi}$. This is physically reasonable since each double pass through the modulator produces an additional frequency shift, as shown in Fig. 3(b).

C. Case 3: phase ramp, $t_1 < T'$

In this case, more than one mode can be generated. The initial condition (12) applies, but the phase ramp

$$\phi(t) = \dot{\phi}t, \quad 0 < t < t_1$$

reaches its final value $\phi = \phi(t_1)$ in less than the round-trip time, $t_1 < T'$. Utilizing (10c) and (10d), the cavity modes in this example have frequencies given by

$$\Omega = \nu\omega/[\nu' + \phi(t_1)/2\pi], \tag{23}$$

where the initial mode prior to switching is $\nu' = \omega T/2\pi$.

In the first round trip, the fields are

$$\begin{aligned} &E(t) = E_0 e^{i(\omega - \dot{\phi})t}, \quad 0 < t < t_1 \\ &E(t) = E_0 e^{[\omega t - \phi(t_1)]}, \quad t_1 < t < T'. \end{aligned} \tag{24}$$

Thereafter, this time dependence repeats periodically in the interval T', consistent with (11). Figure 3(c) shows this periodic phase-time behavior. The Fourier transform of (24) yields the amplitude of the νth mode

$$a_\nu = \frac{E_0}{T'}\left(\frac{e^{i(\omega - \dot{\phi} - \Omega)t_1} - 1}{i(\omega - \dot{\phi} - \Omega)} + \frac{e^{-i\phi(t_1)}}{i(\omega - \nu 2\pi/T')} \times (e^{i\omega T'} - e^{i(\omega - \nu 2\pi/T')t_1})\right), \tag{25}$$

where the cavity frequency Ω is given by (23). It is clear that in the $\lim_{t_1 \to T'} a_\nu = E_0$, in agreement with (18). Also, it is evident that more than one mode now appears.

These few cases illustrate some of the major properties of laser frequency switching and outline how others can be treated as well.

IV. SWITCHING TECHNIQUE

A. Apparatus

The experimental arrangement shown in Fig. 4 consists of a cw dye laser having an intracavity electro-optic phase modulator. A dc electric field ramp pulse applied to a modulator crystal of length z_x induces a time-dependent index change, as described in Eq. (6), producing an optical phase shift

$$\phi(t) = 2(\omega/c)z_x \dot{n} t$$

in an incident beam of angular frequency ω. As explained in Sec. III, the time-dependent phase variation shifts the initial frequency to a new value. Because of the arguments discussed in Sec. II, a resonant sample placed in the path of the external laser beam generates coherent absorption or emission transients in the forward beam. The emerging light is monitored by a fast photodiode and a sampling oscilloscope which is interfaced with a computer for data storage and subsequent data handling.

Electro-optic modulator: The geometry of a Lasermetrics electro-optic phase modulator[14] element is given in Fig. 5. It is an X-cut crystal of ammonium dideuterium phosphate (AD*P). Voltage pulses applied in the X direction induce a significant index change along the E direction only, the polarization direction of the laser beam as shown. The crystal is immersed in an index matching fluid between antireflection coated windows. Insertion of the modulator unit in a cw dye-laser cavity reduces the output power by about 50%.

Pulsers: Various square-wave pulse generators have been used as modulator drivers including

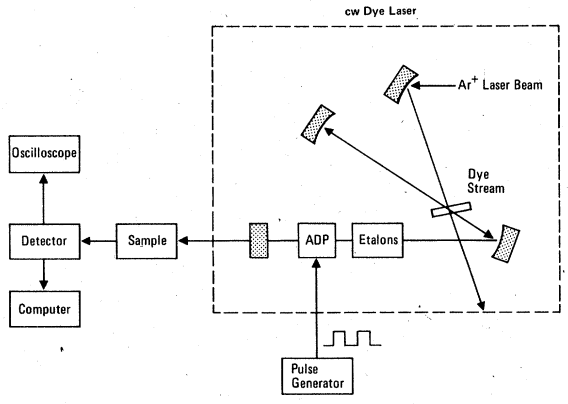

FIG. 4. Schematic of apparatus for observing coherent optical transients using a frequency-switched cw dye laser. Taken from Ref. 3.

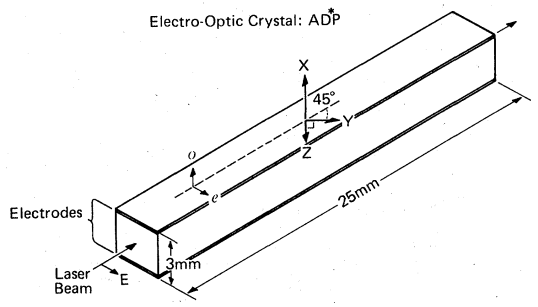

FIG. 5. Geometry of the electro-optic phase-modulator crystal ammonium dideuterium phosphate (AD*P).

the Hewlett-Packard HP 1900A, the HP 214A, and a Huggins pulser where the pulse rise times are 7, 14, and ≤1 nsec, respectively. The first two operate in a single- or a double-pulse sequence and are triggered repetitively at a 25-kHz rate. The third generator produces a 100-nsec square-wave pulse at a 60-Hz repetition rate. Frequency shifts of 0.6 MHz/V are observed in the above modulator, as indicated by the beat frequency of an FID signal of I_2 vapor. The maximum shift detected thus far is about 300 MHz, which compares to the laser's axial-mode spacing of 390 MHz. Above this frequency an additional axial mode is frequently noted.

Laser source: Either a Spectra-Physics 580A or a coherent 599 single-mode cw dye laser is used where the axial-mode spacing is 390 and 283 MHz, respectively. The dye is Rhodamine 6G. The output is linearly polarized and exhibits with the intracavity modulator a maximum power of ~50 mW in a 0.5-mm beam diameter.

Detection: A *P-I-N* photodiode HP 5082-4227 possesses an intrinsic response time of ~1 nsec and is matched to a B and H Electronics Co. preamplifier having a 130-psec response time and 20-dB gain. In most of the work reported here, another preamplifier with ~1 nsec response time and 26-dB gain was used. The detector output is monitored using a Tektronix 7904 oscilloscope with a 7S11 plug in sampling unit and type S-5 or S-4 sampling head having an ultimate response of 1 nsec and 25 psec, respectively. An IBM System 7 computer provides a digital time base which sweeps the time axis of the oscilloscope in steps while sampling and storing the time-averaged signal amplitude point by point. Typically, 1024 data points are swept in a 2-min interval.

B. Performance

A direct measurement of the laser frequency shift is illustrated in Fig. 6. By means of an optical delay

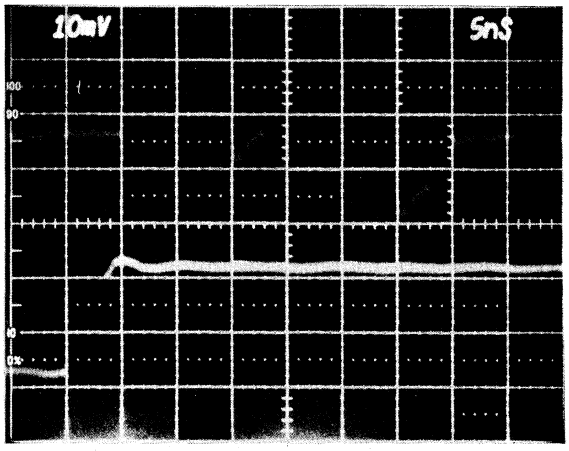

FIG. 6. Direct measurement of laser frequency switching. A 370-V step-function pulse (lower trace) applied to the AD*P modulator produces a 210-MHz laser frequency shift as seen in the heterodyne beat signal (upper trace) of the shifted laser beam and an unshifted component, which is retarded in an optical delay line. The time scale is 5 nsec/division.

line, the unshifted cw laser beam is delayed and then recombined with the frequency-shifted beam to produce a heterodyne beat signal at a photodetector. A beat frequency of 210 MHz, shown in the upper trace, results form a 370-V step-function pulse (lower trace) applied to the AD*P modulator. Note that the beat signal is delayed relative to the voltage pulse because of the time required for light to travel from the laser to the photodetector. The beat signal lasts ~20 nsec because that is the pulse width of the unshifted beam.

Figure 6 shows that the beat signal appears in ~1 nsec, which is the response time of the preamplifier and detector. There is no slow buildup. Clearly, the switching time is not limited by the laser cavity ringing time of ~20 nsec. According to Sec. III and Fig. 3 in particular, the frequency shift occurs instantaneously, but as already mentioned, this conclusion cannot be sustained. The finite length z_x of the modulator introduces a distribution of phase shifts corresponding to different transit times $z_x/c \sim 50$ psec, which is perhaps the limiting response time for this modulator configuration and at present cannot be detected.

Examples of coherent-optical-transient effects are given in Figs. 7–9 for free induction decay (FID), nutation, and the photon echo effect. The sample is I_2 vapor at a pressure of ~30 mTorr, and the transition $(v,J) = 2,59 \rightarrow 15,60$ of $X\,^1\Sigma_g^+ \rightarrow B\,^3\Pi_{0^+u}$ falls in the visible region at 16 956.43 cm^{-1}, ~8 GHz above the lower-frequency sodium D line. Figure 7 is a computer plot of 1024 ex-

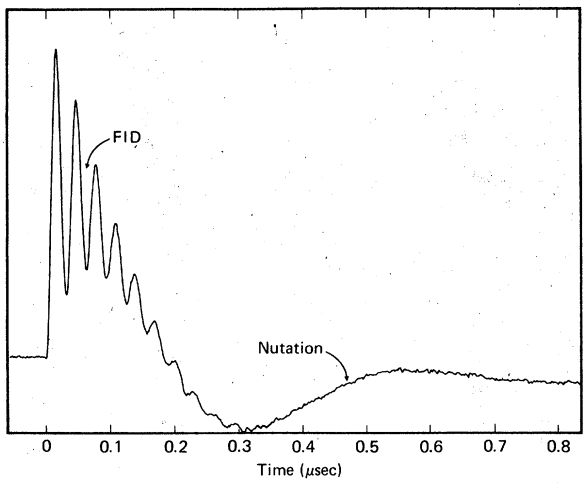

FIG. 7. Computer plot of 1024 experimental points showing the free induction decay and nutation in I_2 vapor at 30 mTorr under conditions where both appear simultaneously. The transition $(v,J)=2,59\rightarrow 15,60$ of $X\,^1\Sigma_g^+ \rightarrow B\,^3\Pi_{0^+u}$ occurs at 16 956.43 cm^{-1}. The dye-laser power is 7 mW and the beat frequency is 32 MHz corresponding to ~ 50-V pulse. For other conditions see Sec. IV.

perimental points which have been stored in a single run. The heterodyne beat frequency of 32 MHz easily distinguishes the FID signal from the slowly varying nutation signal following a step-function switching pulse of ~50 V. Figure 8 shows an FID signal for a ~90-V pulse, the beat frequency being 54 MHz. In Fig. 9, a two-pulse sequence

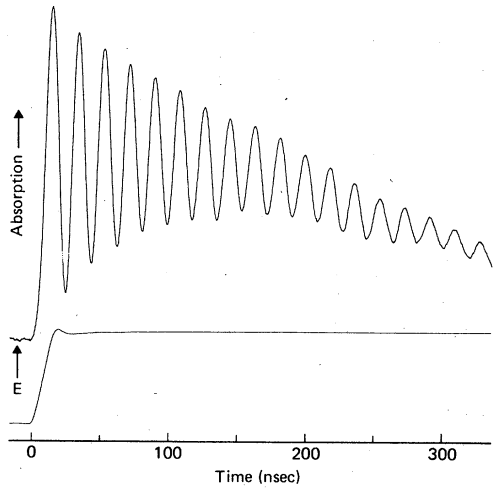

FIG. 8. Free induction decay in I_2 where the laser power is 1.9 mW and the beat frequency is 54 MHz corresponding to ~ 90-V pulse. The nutation frequency is smaller than in Fig. 7 because the laser power is lower.

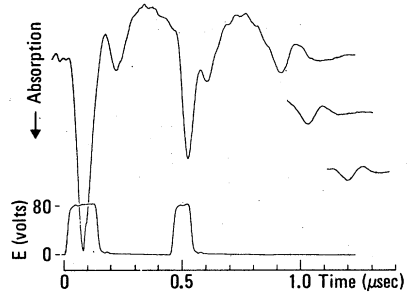

FIG. 9. Photon echoes in I_2 occurring at ~ 1 μsec where the successive echoes decay with increasing pulse delay time following two laser frequency switching pulses. Other conditions are the same as in Fig. 7. Taken from Ref. 3.

results in the photon echo which is shown for three different pulse delay times.

It should be mentioned that laser frequency switching can result in small changes of the laser intensity. This effect is noticeable when the laser frequency is shifted far off the peak of the response curve of the thickest intracavity etalon. Amplitude modulation is minimized by locking the peak transmission point of the intracavity étalon to the laser cavity.

C. Advantages

It is now possible to summarize some of the advantages inherent in the laser-frequency-switching technique. (i) The entire class of coherent-optical-transient effects can be monitored since the electronic pulse sequence can be tailored to the particular experiment of interest. (ii) The dye laser performs a unique role here because its dephasing time is only a few picoseconds and therefore is incapable of generating coherent transients of its own, which on a longer time scale would obscure the measurements. Gas lasers such as the Ar^+ laser are unsuitable, for example, because we have found that they exhibit coherent transients on a ~10-nsec time scale when frequency switched. (iii) The only transient observed is the desired coherent transient itself; this is not the case with pulsed laser sources as the small coherent transient signal often rides on top of the laser pulse and the two are not easily separated. (iv) Heterodyne detection occurs automatically. This identifies the emission signal and increases the signal amplitude by several orders of magnitude. (v) The method is also quite sensitive. Free induction decay signals have been observed at a laser power of 50 μW and with as few as 5×10^5 I_2 molecules. In more strongly absorbing systems and with more efficient signal

averaging, these numbers may be reduced even further. (vi) The method is extremely simple, and while it is similar to the Stark switching technique, the difficulty of being restricted to Stark tunable systems is removed. (vii) Decay-time measurements should be feasible over a very wide range, from milliseconds to ~50 psec. Moreover, when these features are combined with the broad tuning range available in a dye laser, it is apparent that coherent-transient phenomena can now be observed with ease in a large number of optical transitions in various atomic, molecular, and solid state systems.

D. External modulation

When the atomic decay time is less than the round-trip time of light in the laser cavity, intracavity modulation serves no purpose. In this circumstance, the phase modulator might as well be outside the laser cavity. For external modulation, the frequency shift occurs only as long as the modulator's index is time-varying, i.e., as long as the applied modulator voltage continues to change. When the voltage assumes a constant value, the transmitted beam is unshifted.

This mode of operation contrasts with intracavity modulation. In the latter, the frequency-shifted light does not escape primarily into free space, but rather is stored in the cavity. Thus, the laser exhibits memory of the frequency shift. When the modulator voltage reaches a constant value, as discussed in Sec. III, the shift remains constant also. As a result, very long decay times ($T_2 \gg 2L/c$) can be measured, whereas with external modulation the required voltage would be prohibitive. For example, in our FID studies of I_2 vapor a 50-V pulse with a 7.5 nsec rise time produces a 30-MHz shift. In the case where the modulator is external to the laser cavity and assuming that $t_1 = T'$, the same voltage ramp produces the same frequency shift but now the ramp must be maintained over the duration of the experiment, i.e., over the dephasing time T_2 ~1 μsec, and this implies a voltage rise of 6500 V.

E. Telle-Tang modulator

A very different manifestation of rapid electro-optic tuning of a cw dye laser has been introduced by Telle and Tang[15] and perhaps some comparison should be made. In their device, the intracavity electro-optic crystal is driven sinusoidally at exactly twice the axial-mode frequency. The time variation of the modulator's refractive index sweeps the optical cavity length continuously, and hence a distribution of frequencies circulates through the cavity. A rather impressive sweep of ~100 Å in a few nanoseconds has been achieved. However, in this steady-state device, it is not possible to *preselect* a particular frequency in an arbitrary pulse sequence, as in the method described in this article.

V. APPLICATIONS

The coherent optical transients discussed here and in an earlier Letter[3] offer new ways for examining atomic and molecular collisions as well as dephasing mechanisms in solids. These time-dependent interactions which often give rise to a narrow homogeneous line shape can now be extracted from the much broader inhomogeneous profile. In preliminary studies of I_2 vapor,[3] the line-broadening contributions of dephasing and depopulating collisions could be distinguished. Laser frequency switching has been extended also to Na vapor[16] and to impurity ion solids at liquid-helium temperature, such as Pr^{3+} in a LaF_3 host crystal[17] and the F_3^+ center in NaF.[16] In addition, organic mixed crystals such as pentacene in *p*-terphenyl have been examined by this technique.[18,19]

In this section, we wish to emphasize the importance of the FID effect in dephasing studies and examine its characteristics further. For example, in Figs. 7 and 8 we see that the entire decay behavior is obtained conveniently in a single burst, in contrast to an echo experiment where the pulse delay time must be advanced repeatedly. Because of the sensitivity afforded by optical heterodyne detection, weak transitions can be examined, and also, the laser power may be low so that power and inhomogeneous broadening do not seriously affect the decay rate. In comparison, the echo experiments require higher laser intensities where the pulse areas approximate $\frac{1}{2}\pi$.

Free-induction-decay experiments for I_2 are presented here which explore the dependence of the decay rate and amplitude on laser intensity and thus provide a quantitative test of earlier FID theories.[2,21] Precise dephasing times are obtained by Fourier transforming the FID signals, a technique which we now describe.

A. Fourier-transform spectroscopy

In an earlier Letter,[20] Doppler-free infrared spectra were derived from molecular coherent transients using Stark switching and a digital time-frequency Fourier-transform method. Here, the same Fourier technique is adapted to the visible region using laser frequency switching. The spectrum

$$E(\omega) = \frac{1}{\sqrt{(2\pi)}} \int_{-\infty}^{\infty} E(t) e^{i\omega t}\, dt \tag{26}$$

is obtained by Fourier transforming the time-dependent optical field amplitude $E(t)$. For digital evaluation, we replace the integral (26) by the sum

$$E(\omega)=\frac{2}{\sqrt{(2\pi)}}\sum_{n=0}^{N}[E(t)-E(\tau)]\cos\omega t\,, \qquad (27)$$

where

$$t=n\Delta t,\quad n=0,1,2,\ldots$$

$$\omega=I\omega_0,\quad I=0,1,2,\ldots.$$

In the above, τ is the finite duration of the transient signal, Δt is the increment that time advances from one datum point to the next, and thus $N=\tau/\Delta t$ is the number of data points, which in a given experiment are stored in a computer. The frequency $\omega_0=2\pi/\tau$ defines the smallest resolvable interval.

In Eq. (26), we have symmetrized the field about the time origin so that $E(t)=E(-t)$ and therefore only the cosine term need be retained. To truncate the integral and also to avoid a discontinuity in $E(t)$ at $t=\tau$, which otherwise would introduce undesired Fourier components (for example a δ function at the origin $\omega=0$), we have also replaced $E(t)$ by $E(t)-E(\tau)$, making the last point zero. In addition, the time origin of the initial point $E(t=0)$ must be carefully selected from the experimental points otherwise the spectral lines will be partly dispersive rather than absorptive.

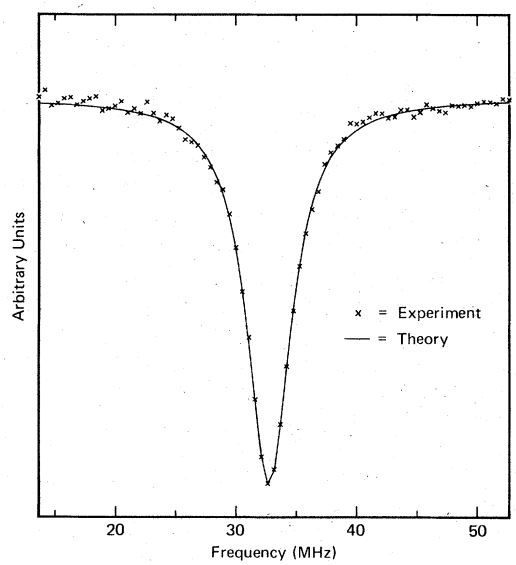

FIG. 10. Computer plot of Fourier-transform spectrum of an I_2 FID-nutation signal similar to Fig. 7. Only the FID portion of the spectrum is shown where the center frequency is 32.83 MHz and the Lorentzian line shape has a FWHM value of 4.11 MHz. The nutation spectrum appears at ~1 MHz. The laser power is 4 mW and other conditions are the same as in Fig. 7.

Figure 10 shows the Fourier transform of a transient signal similar to Fig. 7. Whereas the nutation and FID signals overlap in time they are separable in the frequency domain. The nutation spectrum, which is not shown in Fig. 10, appears at ~1 MHz while the FID line peaks at a beat frequency of ~33 MHz and without any background. Here, the pulse voltage ~50 V. The experimental points (×) closely follow a Lorentzian line shape (solid line) given by the Fourier transform of a damped cosine.

$$E(t)=E_0e^{-\bar{\Gamma}t}\cos\omega t\,.$$

A least-squares fit yields the center frequency

$$\omega/2\pi=32.83\ \text{MHz}\,,$$

and the linewidth at FWHM

$$\omega_{1/2}/\pi=4.11\ \text{MHz}\,,$$

where the dephasing rate $\bar{\Gamma}=\omega_{1/2}$. The high precision of about one part in 400 in the linewidth determination is due to the excellent signal-to-noise ratio of the transient signals and the high data handling capability of computers.

B. Free induction decay

Before proceeding with the FID measurements, we briefly review the results of a recent FID calculation.[21] We assume that the sample is coherently prepared under steady-state conditions and then freely radiates a coherent beam of light after the laser frequency is suddenly switched. Neglecting unimportant factors, the FID heterodyne beat signal for the optical transition $2\rightarrow1$ is of the form

$$\langle E_b^2(t)\rangle\sim\chi^2\left(1-\frac{\Gamma}{(\Gamma^2+\hat{\Gamma}^2)^{1/2}}\right)\times\exp\{-[\Gamma+(\Gamma^2+\hat{\Gamma}^2)^{1/2}]t\}\cos\omega t. \qquad (28)$$

The bracket $\langle\ \rangle$ signifies that an average is performed over the Doppler line shape in the limit where the free induction decay rate

$$\bar{\Gamma}=\Gamma+(\Gamma^2+\hat{\Gamma}^2)^{1/2} \qquad (29)$$

is considerably less than the Doppler width, i.e., $\bar{\Gamma}\ll ku$. Thus, Eq. (29) depends on the dipole dephasing rate

$$\Gamma\equiv1/T_2=\tfrac{1}{2}(\Gamma_1+\Gamma_2)+\Gamma_\phi\,, \qquad (30)$$

and a power-broadening term

$$\hat{\Gamma}^2=(\chi^2\Gamma/2\Gamma_1\Gamma_2)(\Gamma_1+\Gamma_2-\gamma)\,, \qquad (31)$$

where the upper and lower levels, labeled 2 and 1, respectively, depopulate at the rates Γ_2 and Γ_1; the rate of phase interrupting collisions is Γ_ϕ; and γ is the radiative spontaneous emission decay

rate for the $2 \rightarrow 1$ transition. The Rabi frequency is given by $\chi = \mu_{12} E_0/\hbar$ with μ_{12} the transition dipole moment and E_0 the laser field amplitude.

We are now in a position to discuss the dependence of $\langle E_b^2(t)\rangle$ on laser intensity which is given by the preexponential factor of (28),

$$\chi^2[1-\Gamma/(\Gamma^2+\hat{\Gamma}^2)^{1/2}].$$

Clearly, at higher laser intensities when $\hat{\Gamma}^2/\Gamma^2 \gg 1$,

$$\langle E_b^2(t)\rangle \sim \chi^2 e^{-\bar{\Gamma}t}\cos\omega t . \tag{32}$$

At low laser intensities when $\hat{\Gamma}^2/\Gamma^2 \ll 1$,

$$\langle E_b^2(t)\rangle \sim \chi^4 e^{-\bar{\Gamma}t}\cos\omega t + O(\chi^6) + \cdots . \tag{33}$$

In order to test the above theory, the intensity dependence of the FID amplitude $\langle E(t)\rangle$ was measured for I_2 vapor. The experimental conditions were those of Sec. IV, but in addition some care was taken to increase the uniformity of the laser's beam intensity throughout the sample cell. Thus, the beam diameter in the center of the cell was 170 μm and varied longitudinally by 15% or less, where a laser power of 1 mW corresponds to a power density of 2.0 W/cm^2. Figure 11 shows that the observed signal amplitude depends quadratically on the light intensity at low light levels, in agreement with the leading term of (33). Above a laser power of 2 mW, the FID amplitude exhibits a linear intensity dependence and thus follows the limiting behavior (32).

Another verification of the theory can be found in Fig. 12 which shows that the observed FID rate

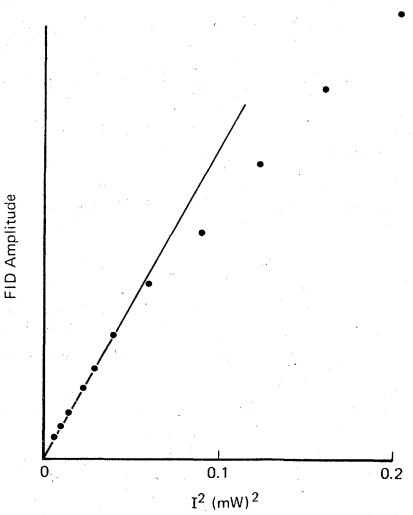

FIG. 11. Amplitude of the observed FID signal of I_2 vs the square of the laser intensity I^2, showing agreement with Eq. (33) in the low-intensity regime. The experimental conditions are given in Fig. 7.

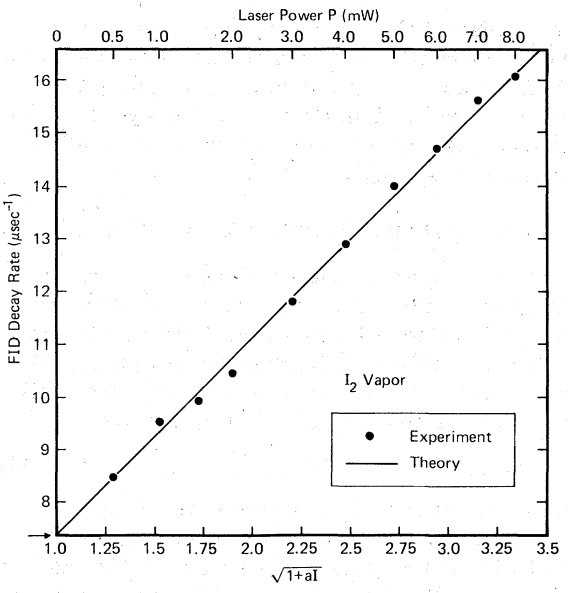

FIG. 12. Free induction decay rate $\bar{\Gamma}$ vs square-root laser-intensity dependence, showing agreement with Eq. (29). Experimental conditions are the same as Fig. 7.

$\bar{\Gamma}$ obeys the square-root intensity dependence predicted by Eq. (29). Here, the decay rate is obtained by the Fourier-transform technique discussed in Sec. V A. Obviously, in the

$$\lim_{\chi \rightarrow 0} \bar{\Gamma} = 2\Gamma \equiv 2/T_2 , \tag{34}$$

and therefore, these measurements allow a determination of the dipole dephasing time T_2.

These results seem to provide the first quantitative and detailed test of the above FID theory.

Finally, we note that (28) does not describe the rapid first order FID because of the approximation $\bar{\Gamma} \ll ku$ adopted in the Doppler average. This problem has been discussed previously in varying stages of approximation[22,23] An analytic result which includes FID and nutation in the weak field limit will be reported subsequently.[24] We have also observed in a high density vapor of either Na or I_2 that a rapid spike appears near the time origin of an FID signal and is quite distinct from the nonlinear heterodyne beat signal shown in Figs. 7 and 8. This new feature may be a manifestation of the first-order FID effect and will require additional study.

ACKNOWLEDGMENTS

We acknowledge with pleasure D. E. Horne for his skillful design of the detector preamplifier, and K. L. Foster for his innovative technical contributions. One of us (R.G.B.) greatly appreciates

the guidance of T. R. Koehler in developing the Fourier-transform program. Conversations with A. E. Siegman on the theory of electro-optic switching were illuminating and timely. This research was supported in part by the U.S. office of Naval Research.

APPENDIX: MOVING-MIRROR MODEL

We wish to show that when one end mirror of an optical cavity is set into uniform motion, the initial mode exhibits a Doppler shift that is equivalent to electro-optic frequency switching. The cavity geometry of Fig. 2 is assumed. We shall examine the behavior of the running wave

$$E = E_0 e^{i(\omega t - kz)}, \quad t < 0 \tag{A1}$$

at the position $z = 0$ where the initial frequency $\omega = \nu 2\pi/T$. The end mirror, located initially at $z = 0$, is set into uniform motion at $t = 0$ in the negative z direction with velocity v and comes to a stop at $t = t_1$.

The light wave reaching $z = 0$ after reflection by the moving mirror travels the additional distance $\Delta z = 2vt$ and thus is retarded in phase by

$$\begin{aligned} \phi(t) &= k\Delta z = 2kvt, \quad 0 < t < t_1 \\ \phi(t) &= 2kvt_1, \quad t_1 < t < T'. \end{aligned} \tag{A2}$$

The modulated field during the first round-trip interval becomes

$$\begin{aligned} E(t) &= E_0 e^{i(\omega - 2kv)t}, \quad 0 < t < t_1 \\ E(t) &= E_0 e^{i(\omega t - 2kvt_1)}, \quad t_1 < t < T'. \end{aligned} \tag{A3}$$

It is also evident that the new cavity round trip time is

$$T' = T + (2v/c)t_1, \tag{A4}$$

and the frequency of the νth mode is

$$\Omega = \nu 2\pi/T'. \tag{A5}$$

The Fourier amplitudes can now be obtained for the various modes ν using (A3)–(A5) and (10).

For the case that $t_1 = T'$, the amplitudes

$$\begin{aligned} a_\nu &= E_0, \quad \nu = (\omega - 2kv)/(2\pi/T') \\ a_\nu &= 0, \quad \nu = (\omega - 2kv)/(2\pi/T') \pm 1, \pm 2, \pm 3, \ldots . \end{aligned} \tag{A6}$$

Thus, the initial mode $\nu = \omega T/2\pi$ persists where the new frequency

$$\Omega = \omega - 2kv = \omega(1 - 2v/c) \tag{A7}$$

is Doppler shifted to lower frequencies by $(2v/c)\omega$. The factor of 2 arises in (A7) because the light wave reverses direction upon reflection. With the Doppler shift $2kv$ replacing $\dot{\phi}$ in (15), it is clear that this mechanical model is equivalent to electro-optic frequency switching.

[1] N. A. Kurnit, I. D. Abella and S. R. Hartmann, Phys. Rev. Lett. 13, 567 (1964); I. D. Abella, N. A. Kurnit and S. R. Hartmann, Phys. Rev. 141, 391 (1966).

[2] R. G. Brewer and R. L. Shoemaker, Phys. Rev. A 6, 2001 (1972).

[3] R. G. Brewer and A. Z. Genack, Phys. Rev. Lett. 36, 959 (1976).

[4] R. G. Brewer, Physics Today 30, No. 5, 50 (1977).

[5] A. Abragam, *The Principles of Nuclear Magnetism* (Oxford, London, 1961).

[6] I. P. Kaminow, *An Introduction to Electro-optic Devices* (Academic, New York, 1974).

[7] R. G. Brewer, in *Frontiers in Laser Spectroscopy*, edited by R. Balian, S. Haroche, and S. Liberman (North-Holland, Amsterdam, 1977), Vol. 1, p. 341.

[8] R. G. Brewer, in NATO Advanced Study Institute on Coherence in Spectroscopy and Modern Physics, edited by F. T. Arecchi (Plenum, New York, to be published).

[9] R. G. Brewer and R. L. Shoemaker, Phys. Rev. Lett. 27, 631 (1971).

[10] P. P. Sorokin and J. P. Lankard, IBM J. Res. Dev. 10, 162 (1966); F. P. Schafer, W. Schmidt, and J. Vloze, Appl. Phys. Lett. 9, 306 (1966).

[11] J. L. Hall, in *Atomic Physics*, edited by S. J. Smith, G. K. Walters and L. H. Volsky (Plenum, New York, 1973), p. 615.

[12] A. Yariv, IEEE 52, 719 (1964).

[13] A. Schenzle and R. G. Brewer (unpublished).

[14] D. Anafi, R. Goldstein, and J. Machewirth, Laser Focus, 13, 72 (1977).

[15] J. M. Telle and C. L. Tang, Appl. Phys. Lett. 26, 572 (1975).

[16] R. M. Macfarlane, A. Z. Genack, and R. G. Brewer, Phys. Rev. B (to be published).

[17] A. Z. Genack, R. M. Macfarlane and R. G. Brewer, Phys. Rev. Lett. 37, 1078 (1976).

[18] A. H. Zewail, T. E. Orlowski and K. E. Jones, Proc. Natl. Acad. Sci. USA 74, 1310 (1977); Spectrosc. Lett. 10, 115 (1977).

[19] D. A. Wiersma, in Eighth Molecular Crystal Symposium, Santa Barbara, California, May 29–June 2, 1977 (unpublished); H. de Vries, P. de Bree, and D. A. Wiersma, Chem. Phys. Lett. 52, 399 (1977).

[20] S. B. Grossman, A. Schenzle, and R. G. Brewer, Phys. Rev. Lett. 38, 275 (1977).

[21] A. Schenzle and R. G. Brewer, Phys. Rev. A 14, 1756 (1976).

[22] K. L. Foster, S. Stenholm, and R. G. Brewer, Phys. Rev. A 10, 2318 (1974).

[23] P. F. Liao, J. E. Bjorkhohn, and J. P. Gordon, Phys. Rev. 39, 15 (1977).

[24] R. G. DeVoe and R. G. Brewer, Bull. Am. Phys. Soc. 23, 75 (1978).

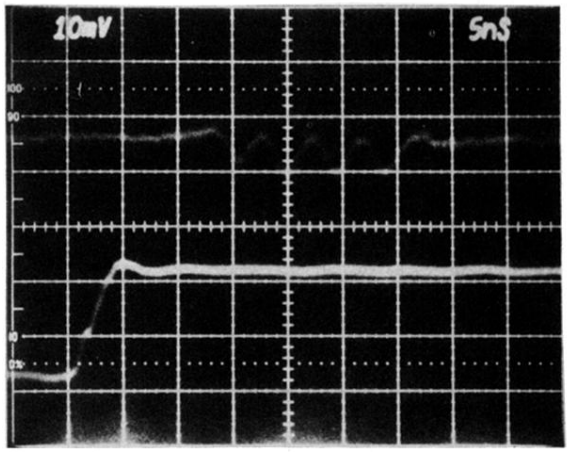

FIG. 6. Direct measurement of laser frequency switching. A 370-V step-function pulse (lower trace) applied to the AD*P modulator produces a 210-MHz laser frequency shift as seen in the heterodyne beat signal (upper trace) of the shifted laser beam and an unshifted component, which is retarded in an optical delay line. The time scale is 5 nsec/division.